Tracking age differences in neural distinctiveness across representational levels

Malte Kobelt[1,2,5], Verena R. Sommer[1,5], Attila Keresztes[3,4], Markus Werkle-Bergner[1,6], & Myriam C. Sander[1,6,7]

[1] *Center for Lifespan Psychology, Max Planck Institute for Human Development, 14195 Berlin, Germany*
[2] *Institute of Cognitive Neuroscience, Ruhr-Universität Bochum, 44780 Bochum, Germany*
[3] *Brain Imaging Centre, Research Centre for Natural Sciences, 1519 Budapest, Hungary*
[4] *Faculty of Education and Psychology, Eötvös Loránd University, 1053 Budapest, Hungary*

[5] *These authors contributed equally*
[6] *Senior authors*
[7] *Lead Contact*

Correspondence concerning this article should be addressed to:
Myriam C. Sander (sander@mpib-berlin.mpg.de) or Markus Werkle-Bergner (werkle@mpib-berlin.mpg.de)
Lead contact: Myriam C. Sander (sander@mpib-berlin.mpg.de)

Summary

The distinctiveness of neural information representation is crucial for successful memory performance but declines with advancing age. Computational models implicate age-related neural dedifferentiation on the level of item representations, but previous studies mostly focused on age differences of categorical information representation in higher-order visual regions. In an age-comparative fMRI study, we combined univariate analyses and whole-brain searchlight pattern similarity analyses to elucidate age differences in neural distinctiveness at both category and item levels and their relation to memory. Age-related neural dedifferentiation was shown as reduced category-selective processing in ventral visual cortex and impoverished item specificity in occipital regions. Importantly, successful subsequent memory performance built upon high item stability which was greater in younger than older adults. Finally, we identified a multivariate profile of neural distinctiveness across representational levels that captured both age group and recognition performance differences, emphasizing that neural dedifferentiation is a generalized phenomenon in the aging brain.

Key words: episodic memory, aging, neural distinctiveness, neural dedifferentiation, representational similarity, fMRI

Introduction

A prominent theory of cognitive aging assumes that neural representations become less distinctive in old age and that this so-called neural dedifferentiation underlies age-related cognitive impairments (e.g., Koen and Rugg, 2019; Li et al., 2001; Park et al., 2010). In computational models, age differences have been ascribed to deficient neuromodulation that causes haphazard activation to identical informational input leading to lower stability (i.e., consistency of neural activity across repetitions) of representations on the item level as well as increasing random activation variability within the network leading to a decrease in the distinctiveness of the network's representations (Li and Sikström, 2002; Li et al., 2000, 2001). Importantly, deficient neuromodulation thus results in age differences in neural information representation that coexist at various levels, i.e., at the level of item representations and the level of category representations, and jointly affect memory performance. However, previous age-comparative studies (mainly using functional magnetic resonance imaging; fMRI) have nearly exclusively focused on age-related dedifferentiation in categorical representations, neglecting age differences at the level of item representations that possibly occur already during earlier stages of visual processing. Hence, while long-standing observations from behavioral

aging research suggest a close connection between age differences in sensory processing and decline in higher order cognition (e.g., Baltes and Lindenberger, 1997; Li and Lindenberger, 2002; Lindenberger and Baltes, 1994; Schneider and Pichora-Fuller, 2000), the limited available evidence has not yet allowed to settle the debate whether or not age differences in neural distinctiveness already exist at the level of item representations (Koen and Rugg, 2019). We therefore set out to track age differences at different representational levels, ranging from item-level specificity to category selectivity, with the goal to delineate their unique and joint contribution to memory performance in younger and older adults.

The available evidence clearly supports the notion of age-related neural dedifferentiation of category information. Focusing on age differences in the representation of broader categories such as faces, houses, or objects within the ventral visual cortex (VVC; Koen et al., 2019; Park et al., 2004, 2012; Payer et al., 2006; Srokova et al., 2020; Voss et al., 2008), previous studies made use of the preferential response of these regions to specific stimulus categories (Epstein and Kanwisher, 1998; Grill-Spector and Malach, 2004; Kanwisher et al., 1997). For example, using conventional univariate analyses, Park et al. (2004) demonstrated that, compared to young adults, older adults exhibited less category-selective blood oxygen level dependent (BOLD) responses to stimuli of faces, houses, chairs, and pseudowords, providing the first human evidence for age-related neural dedifferentiation in the VVC (see also Park et al., 2012; Payer et al., 2006, and, accounting for trial-wise BOLD variability: Koen et al., 2019; Voss et al., 2008). Directly probing the (dis-)similarity of distributed, multivariate activation patterns – with representational similarity (cf. Edelman, 1998; Kriegeskorte et al., 2008) or decoding techniques (cf. Haynes and Rees, 2006; Mur et al., 2009) – subsequent studies revealed that different stimulus categories were represented less distinctively in category-selective areas in the VVC in older compared with younger adults (Carp et al., 2011; Koen et al., 2019; Park et al., 2010; Trelle et al., 2019). A few age-comparative studies also investigated neural distinctiveness at the within-category (Goh et al., 2010) or even item level (Trelle et al., 2019). Unfortunately, with few exceptions (Sommer et al., 2019; St-Laurent et al., 2014), these studies focused on predefined category-specific regions. However, it is very likely that processing of item-specific representations is also supported by other brain regions than those showing category selectivity (see e.g., Kriegeskorte et al., 2007). We therefore speculated that age differences in item specificity may have gone unnoticed in most studies with region-of-interest (ROI) approaches that focused on category-specific brain regions.

Importantly, assuming that an altered signal-to-noise ratio in neural information processing leads to more variable neural responses in old age (Li et al., 2001), item-level

specificity in older adults may depend critically on item stability, that is, the consistency with which individual items are represented across several instances of encoding. However, while studies with young-adults-only samples have already revealed the importance of item stability (inside and outside of category-selective areas including, for instance, occipital cortex) for memory performance (Ward et al., 2013, Xue et al., 2010), so far only one study by Zheng et al. (2018) compared item stability across repeated encoding between younger and older adults. They found that, independent of their distinctiveness from other representations, item stability in the visual cortex was reduced in older adults and was associated with lower memory performance compared with young adults. Moreover, item stability was an important contributor to memory performance as indicated by subsequent memory effects (cf. Paller and Wagner, 2002). However, age differences were less clear regarding item specificity, a measure calculated similarly to item stability but corrected for similarity of items from the same category. This inconsistency provoked criticism regarding the validity of the results (see Koen and Rugg, 2019).

In sum, there is a clear tension between model-derived predictions for neural dedifferentiation and available empirical support. While many studies provided coherent evidence for neural dedifferentiation with age at the category level (for reviews, see Koen and Rugg, 2019; Koen et al., 2020), they did not directly test a central tenet of computational models of dedifferentiation (Li and Sikström, 2002; Li et al., 2000, 2001), namely reduced distinctiveness of single-item representations. Thus, whether age differences exist at the level of item representations is an ongoing debate in the field based on highly limited evidence (see e.g., Koen and Rugg, 2019). Hence, in the current age-comparative fMRI study, we combined conventional ROI-based univariate analysis and whole-brain searchlight pattern similarity analysis to elucidate age-related differences in neural specificity both at the level of categorical information as well as at the level of the individual items, and their relation to memory performance.

Results

Behavioral Results

Healthy young adults (n = 35, age: M = 22.11, SD = 2.70, 18–27 years) and older adults (n = 32, age: M = 70.72, SD = 2.26, 67–75 years) incidentally encoded images of faces and houses, followed by a surprise recognition test (see Figure 1A). During encoding, all images were presented twice, namely once in each of two subsequent runs. To ensure adequate processing of the presented face and house images, participants performed a low-level vigilance task during encoding (i.e., pressing a button whenever an interspersed pre-defined target image appeared). Both younger and older participants performed near ceiling in the vigilance task (percentage of correct answers: M_{young} = 98.95%, SD_{young} = 4.69% M_{old} = 98.77%, SD_{old} = 3.54%), reflecting high engagement with the encoding task. Memory performance in the recognition task was assessed by the discrimination-index Pr calculated as the difference between the hit-rate and false-alarm-rate which can range from –1 to 1 with 0 representing chance level. In both age groups, the mean memory performance exceeded chance level (Pr_{young} = 0.24, $t_{\text{young}}(34)$ = 12.18, p_{young} < .001, d_{young} = 2.06, Pr_{old} = 0.19, $t_{\text{old}}(31)$ = 9.16, p_{old} < .001, d_{old} = 1.62) and did not differ between face and house images (faces: Pr_{young} = 0.23, houses: Pr_{young} = 0.25, $t_{\text{young}}(35)$ = 0.93, p_{young} = .358, faces: Pr_{old} = 0.17, houses: Pr_{old} = 0.21, $t_{\text{old}}(31)$ = 1.67, p_{old} = .105). Older adults gave more "old" responses for both previously learned (hit-rate$_{young}$ = 0.50, hit-rate$_{old}$ = 0.61, $t(65)$ = –3.08, p = .003, d = 0.75) and completely new images compared to younger adults (false-alarm-rate$_{young}$ = 0.26; false-alarm-rate$_{old}$ = 0.41; $t(65)$ = –4.92, p < .001, d = 1.34). An independent samples t-test revealed no significant difference in memory performance (Pr) between age groups ($t(65)$ = 1.62, p = .110, d = 0.40).

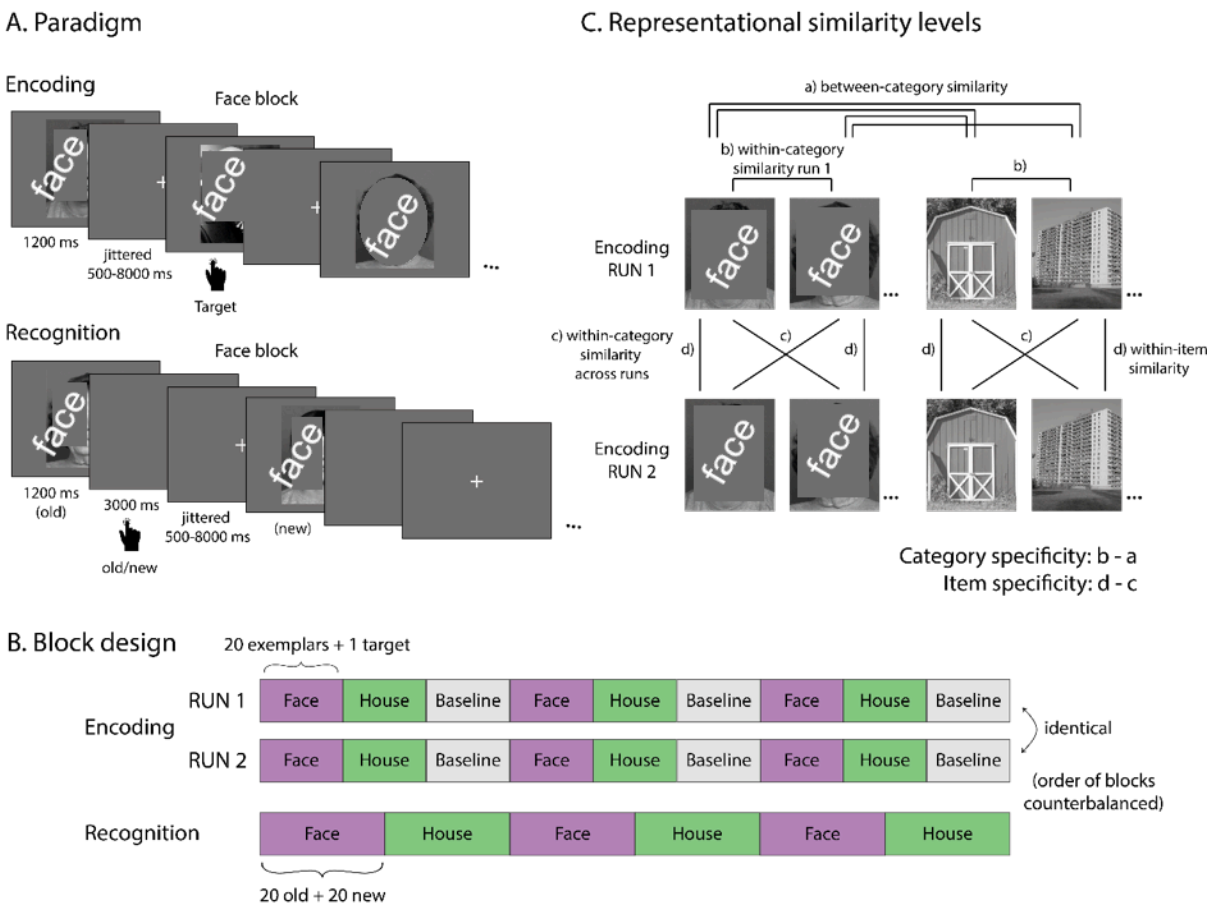

Figure 1. Task design and schematic of representational similarity levels.
A. The paradigm comprised an encoding (top) and recognition (bottom) task. During encoding, participants were asked to press a button whenever a previously trained target image appeared. During recognition, participants responded via button press whether each presented image was old or new. Here, only sample stimuli from a face block are shown for illustration but also houses and baseline control stimuli were presented. Note that the original pictures of faces are covered due to biorxiv regulations. **B.** Illustration of the block design of encoding and recognition tasks. The encoding task consisted of two identical runs, each of which comprised 3 face, 3 house, and 3 baseline (phase-scrambled faces and houses) blocks in alternating and counterbalanced order (either starting with a face or house block). In each block, 20 exemplars of the respective category (face, house, baseline) were presented plus one target stimulus. The recognition task consisted of 3 face and 3 house blocks in alternating and counterbalanced order. In each block, 20 old and 20 new faces/houses were presented. **C.** Simplified illustration of the computed representational similarity levels. For each item presented in encoding run 1, neural pattern similarity was computed as the Pearson correlation of the BOLD pattern elicited by that item and the BOLD pattern(s) elicited by (a) all items of the respective other category in run 1 (between-category similarity), (b) all other items of the same category in run 1 (within-category similarity in run 1), (c) all other items of the same category in run 2 (within-category similarity across runs), (d) the same item in run 2 (within-item similarity; stability). For each subject, the respective similarity measure was averaged across items, resulting in one similarity value for each representational level. Category representation specificity was calculated as the difference of between-category and within-category similarity (b–a). Item representation specificity was calculated as the difference of within-category (across runs) and within-item similarity (d–c). These similarities were assessed based on regions of interests as well as a searchlight approach, see main text.

Category-selective processing in the VVC differs between age groups and is related to memory performance.

Age-related neural dedifferentiation has previously been described as less distinct recruitment of category-selective areas located in the VVC (Park et al. 2004). Using a cluster-based approach (see Methods), we defined two ROIs (see Figure 2) in the bilateral VVC showing the

highest BOLD response to images of faces compared to phase-scrambled control images (face-selective ROI) and to houses compared to control images (house-selective ROI). Within these category-selective functional ROIs, we calculated a *category selectivity score* as the difference in BOLD responses to images of the preferred versus the non-preferred category (e.g., the difference in BOLD responses to images of faces versus houses in the face-selective ROI) during the first encoding run. During encoding, a 2 (Age Group) × 2 (ROI) mixed factorial ANOVA revealed that older adults showed reduced category-selective processing compared to young adults ($F(1,65) = 12.59$, $p < .001$; see Figure 3A). Furthermore, the magnitude of the selectivity score did not differ between ROIs ($F(1,65) = 0.22$, $p = .643$) and there was no interaction between ROI and age ($F(1,65) = 0.06$, $p = .813$). Thus, replicating previous observations (Park et al., 2004; Koen et al., 2019), our findings emphasize that older adults engage category-selective areas in the VVC less distinctively compared to younger adults when encoding visual information.

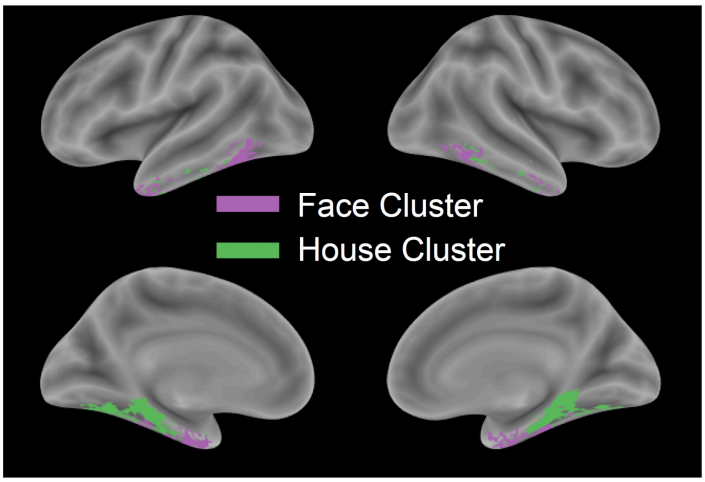

Figure 2. Identification of category-selective clusters in VVC
Surface rendered illustration of non-overlapping category-selective ROIs across all participants. Purple color indicates face-selective ROI. Green color depicts house-selective ROI. Notably, the face-selective ROI is predominantly located in the lateral ventral visual cortex and the house-selective ROI in the medial VVC closely resembling the category-selective areas observed by Park et al. (2012).

If neural dedifferentiation occurred due to age-related increases of haphazard neural activation as claimed by Li and colleagues (2001), lower category selectivity should result from increased neural noise reflected in increased responses to images of the non-preferred category in older adults (i.e., neural broadening, Park et al., 2012). However, the current evidence is fairly mixed as there are studies supporting neural broadening and studies showing the opposite effect – reduced neural responses to images of the preferred category (i.e., neural attenuation; for review see Koen and Rugg, 2019). To unravel whether age-related reductions in category-

selective processing occurred due to a) neural broadening, b) neural attenuation, or c) a mixture of both processes (see Park et al., 2012), we conducted post hoc *t*-tests and used Bonferroni correction to control for multiple comparisons (see Figure 3B). Across ROIs, older adults showed increased BOLD responses to images of the non-preferred category compared to younger adults ($t(65) = 2.38$, $p = .040$), whereas BOLD responses to preferred images did not differ between age groups ($t(65) = -1.13$, $p = .526$). Hence, the observed age-related neural dedifferentiation in category processing most likely resulted from an increased engagement of category-specific regions by non-preferred stimuli in line with the theoretical assumption that broadening effects of the neural tuning curve underlie the loss of neural distinctiveness in older adults (Li et al., 2001).

To test whether interindividual variability in category-selective processing was related to memory performance in the recognition task, zero-order and partial correlations were computed across participants using Pearson's *r*. Selectivity scores were averaged across face and house selective ROIs in the VVC. Across participants, selectivity scores were related to memory performance ($r = 0.34$, $p = .005$; see Figure 3C). Importantly, this correlation remained significant when controlling for age group using partial correlations ($r = 0.29$, $p = .019$). Thus, dedifferentiated visual processing in category-selective areas, as primarily observed in older adults, was related to poorer memory performance independent of age.

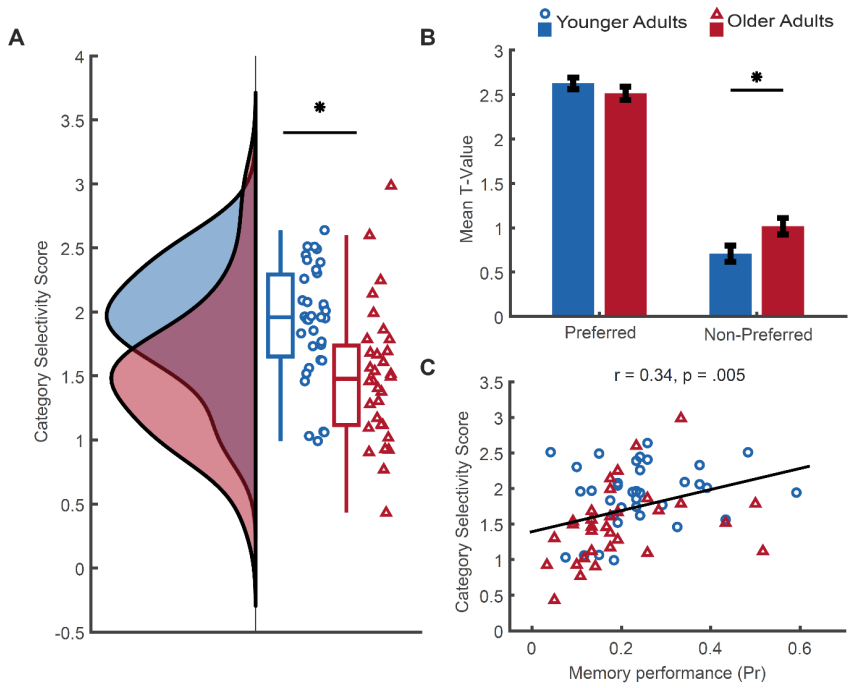

Figure 3. Age differences in category-selective processing during encoding
A. Selectivity score for younger adults (blue; circles) and older adults (red; triangles). Group distributions shown as unmirrored violin plot and boxplots with medians and 95% confidence interval with whiskers representing 2nd

and 98th percentiles (Allen et al., 2018). **B.** Neural response to preferred and non-preferred categories within functionally defined VVC ROIs. The neural response is expressed as the averaged *t*-values for preferred/non-preferred categories against phase-scrambled images within the respective ROIs. Error bars indicate standard error of the mean. **C.** Scatterplot illustrating the association between selectivity scores and corrected recognition (*Pr*) over all participants independent of age. Each circle/triangle represents an individual younger/older adult. For illustrative purposes, the best fitting least-squares line is plotted. Significant group differences ($p < .05$) are indicated by asterisk.

Age differences in category representation specificity are restricted to the VVC

Since category selectivity as assessed with univariate methods relies on averaged BOLD signal changes and does not allow to quantify the distinctiveness of specific item representations, we next used pattern similarity analysis (Kriegeskorte et al., 2008) to investigate the categorical specificity of item representations. This analysis still focusses on differences on the categorical level but uses item-level information instead of averaged activation differences. Thus, we defined the specificity of neural category representations (*category specificity*) as the difference of within-category similarity and between-category similarity (cf. Carp et al., 2011). Similarity indices were based on Fisher *z*-transformed Pearson correlations between single trial beta weights calculated across voxels (Koen et al., 2019).

First, we focused on the category-selective ROIs as defined in the univariate analyses, following an approach widely used in previous studies (Carp et al., 2011; Koen et al., 2019; Trelle et al., 2019). Within each ROI, within-category similarity was computed as the mean similarity between neural patterns evoked by different images of the same preferred category, whereas between-category similarity was defined as the mean similarity of neural activity patterns of images from the preferred to the non-preferred category (see Figure 1C). For example, for the face area, within-category similarity for each participant was calculated as the mean correlation between all face trials whereas between-category similarity was defined as the mean correlation of all face trials to all house trials. Therefore, a larger difference between within- and between-category similarity reflects more distinct neural category representations for the preferred category within each ROI, i.e. higher category specificity.

We used a 2 (Age Group) × 2 (within vs. between-category similarity) × 2 (ROI) mixed factorial ANOVA to investigate age differences in the specificity of neural category representations. Across age groups, within-category similarity was higher than between-category similarity ($F(1,65) = 146.70$, $p < .001$; see Figure 4A). Moreover, the difference between within- and between-category similarity differed by Age Group ($F(1,65) = 4.85$, $p = .031$) indicating lower category specificity in older than younger adults. Neither the main effects of age ($F(1,65) = 2.07$, $p = .155$) or ROI ($F(1,65) = 0.05$, $p = .820$) nor any further interactions reached significance (*ps* > .268).

In contrast to most previous studies which restricted their analyses on category-selective areas in the VVC, we used a searchlight approach to explore age differences in category specificity across the whole brain (Nili et al., 2014). For each voxel in the brain, we calculated the specificity of neural category representations as the difference of within-category similarity and between-category similarity for faces and houses within an 8 mm-radius sphere centered on that voxel. To control for multiple comparisons, we used cluster-based permutation statistics to compare category specificity between age groups (see Methods). In contrast to the ROI analysis, whole-brain analyses revealed no group differences in category specificity for houses ($p > .336$) and furthermore indicated that older adults showed higher category specificity for faces in the superior temporal gyrus ($p = .006$). Thus, while the ROI-based multivariate approach provided evidence supporting age differences in category specificity as reported by several previous studies (Carp et al., 2011; Koen et al., 2019; Trelle et al., 2019), the whole brain approach did not. This result indicates that an age-related decline for category information may be restricted to category-specific brain regions and less pronounced than thought, such that it does not survive exploratory whole brain analyses.

We also tested whether interindividual differences in the specificity of neural category representations in category-specific brain regions were related to memory performance across participants (see Figure 4B). Specificity of neural category representations was calculated as the difference of within- and between-category similarity averaged over face and house selective areas. Neural category representation specificity was not related to memory performance using zero-order ($r = 0.03$, $p = .829$) or partial Pearson correlations controlling for age ($r = -0.03$, $p = .829$). Thus, we found no evidence that the specificity of neural category representations was related to memory performance.

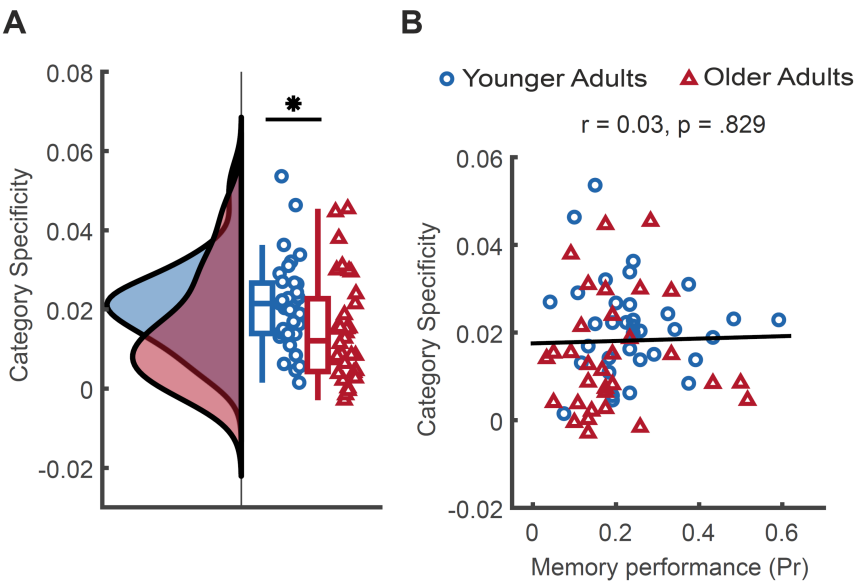

Figure 4. Category representation specificity in the VVC
A. Category specificity calculated as the difference between within- and between-category similarity for younger adults (blue; circles) and older adults (red; triangles). Group distributions as unmirrored violin plot and boxplots with medians and 95% confidence interval with whiskers representing 2nd and 98th percentiles. **B.** Pearson correlation of category specificity and corrected recognition (*Pr*) across subjects. For illustrative purposes, the best fitting least-squares line is plotted. Significant group differences ($p < .05$) are indicated by asterisk.

Item representation specificity in occipital regions is reduced in older adults and linked to memory performance

In contrast to previous studies (Carp et al., 2011; Koen et al., 2019) our results only partially support lower *category specificity* in older adults (namely, when restricting the analyses to category-specific ROIs). However, theoretical accounts based on computational models emphasize that age-related dedifferentiation is particularly reflected in reduced specificity of neural representations of *individual items* (Li et al., 2001) which are not restricted to category-selective areas but are found in large-scale neural networks (Xue, 2018). Therefore, we applied pattern similarity analyses across the whole brain to investigate age-related changes in neural *item specificity*.

Similar to the previously described searchlight analysis on category level, we defined an 8 mm-radius sphere around each voxel. Within each sphere, within-item similarity was calculated as the similarity of neural activity patterns across the two repetitions of a given item (i.e., *item stability;* see Figure 1C). We compared this item stability to the respective within-category similarity to capture the specificity of neural item representations (i.e., *item specificity*). To control for potential confounds due to item repetition, we calculated within-category similarity as the similarity between different images of the same category of different runs. Cluster-based permutation statistics were used to compare item specificity between age groups for face and house images separately. For faces, older adults showed smaller item

specificity compared to younger adults in occipital regions ($p < .001$) including bilateral intracalcarine cortex, lateral occipital cortex and occipital fusiform cortex (see Figure 5A). For houses, older adults also showed smaller item specificity than younger adults in occipital areas ($p = .006$) comprising bilateral lingual gyrus, intracalcarine cortex and left occipital fusiform cortex (see Figure 5B). Thus, our findings underline that older adults form less specific item representations in occipital areas than younger adults.

We also tested whether interindividual differences in *item specificity* were related to overall memory performance (see Figure 5C). For this analysis, we averaged item specificity over both categories in their respective occipital clusters. Neural item representation specificity was related to memory performance using zero-order ($r = 0.39$, $p = .001$) and partial Pearson correlations controlling for age ($r = 0.35$, $p = .004$). Thus, high item representation specificity accounts for interindividual differences in memory performance of younger and older adults.

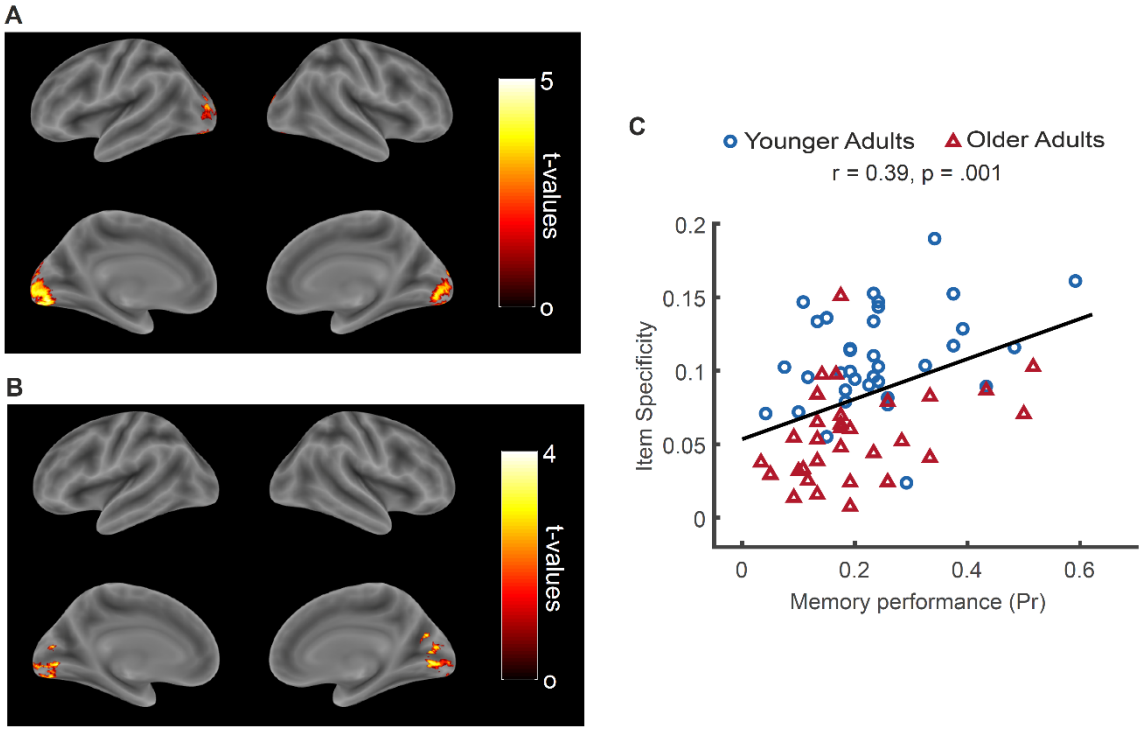

Figure 5. Age differences in item representation specificity and relation to memory performance
A. Significant age differences in item specificity, calculated as the difference between similarity of neural activity patterns across the two repetitions of a given item (i.e., *item stability)* and the respective within-category similarity, for faces indicated by t-values. Younger adults showed higher item specificity in occipital areas compared to older adults as depicted by the presented cluster. **B.** Significant age differences in item specificity for houses. Again, younger adults showed higher item specificity in occipital areas than older adults. **C.** Pearson correlation of item specificity and corrected recognition (*Pr*) over all subjects (younger adults: blue circles; older adults: red triangles).

A specific profile of neural dedifferentiation across representational levels is associated with age and memory performance

Given the coexistence of age differences in *category selectivity, category specificity,* and *item specificity* and their joint contribution to memory performance, we used partial least squares correlation (PLSC) analysis to extract a single composite score that optimally represented the association between participants' age, memory performance, and the multivariate pattern of neural dedifferentiation measures – the *distinctiveness score*. Our PLSC analysis identified a single reliable latent variable (LV; $P < .001$; see Figure 6A) that optimally represented the association between participants' multivariate pattern of neural distinctiveness and (inverted) age ($r = 0.65$; see Figure 6B) as well as memory performance ($r = 0.41$; see Figure 6C). Bootstrap ratios (BSR) indicated that younger age and higher memory performance were mainly associated with higher *category selectivity* (BSR = 5.13), and higher *item specificity* (BSR = 8.03) as the two stable components of the LV, but not *category specificity* (BSR = 1.98). Importantly, in line with our proposal that *item specificity* is an important factor for age and performance differences, *item specificity* was by far the most stable predictor of age and performance differences.

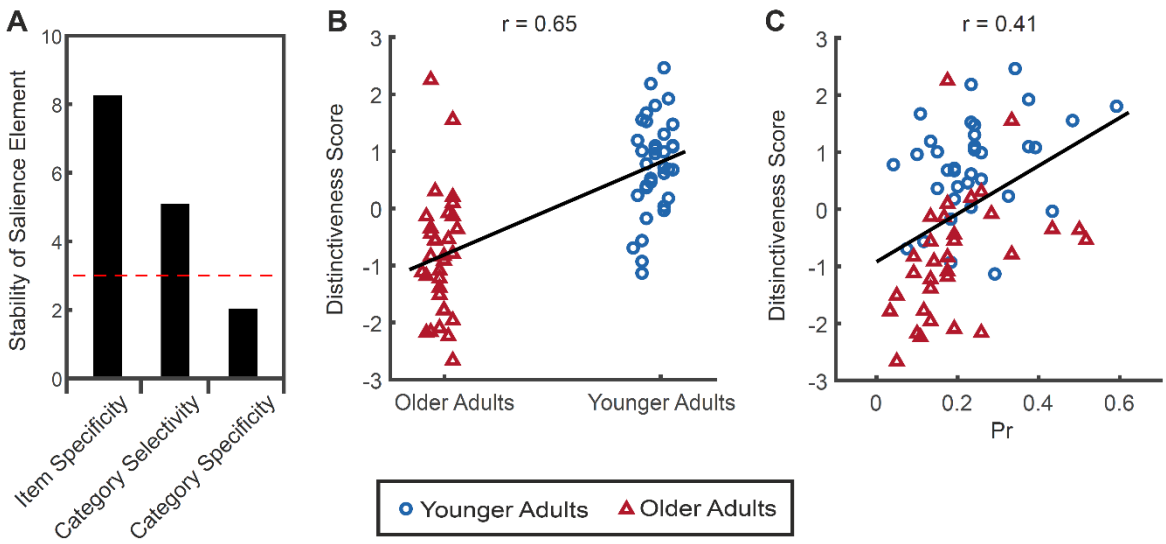

Figure 6. A specific profile of neural distinctiveness across representational levels is associated with age and memory performance

A. Profile of latent variable weights (i.e., "brain saliences", e.g., McIntosh et al., 1996) across three neural distinctiveness levels. Red dashed line indicates significance threshold for latent variable weights after multiple error correction. *Z* score-like values of stability suggest a positive relationship between distinctiveness levels as well as age and memory mostly pronounced for occipital item specificity. Using latent variable weights to transform individual empirical distinctiveness measures results in a single latent variable score expressing the largest amount of shared variance between the multivariate pattern of distinctiveness levels as well as age and memory. **B.** In the optimal solution (see Methods), the resulting latent distinctiveness score is positively related to inverted age and **C** memory performance (*Pr*) meaning that higher expression of the distinctiveness profile is related to higher age and worse memory performance (younger adults: blue circles; older adults: red triangles). Note: Age is inverted (the higher the value the younger the participant) in order to create consistent directionality between all variables of interest; see Methods.

Age and performance differences in occipital item specificity are driven by item stability

Our PLSC analysis revealed that differences in *item specificity* account for the largest variance in age differences as well as interindividual differences in memory performance. Importantly, if, as assumed by Li et al. (2001), more variable neural responses are at the core of age-related reductions in neural specificity, *item specificity* in older adults depends critically on the consistency with which individual items are represented across several instances of encoding, that is, *item stability*. To test whether lower *item specificity* in older adults was indeed due to lower *item stability* (within-item similarity) or higher between-item (within-category) similarity compared to younger adults and whether specifically higher *item stability* was related to a higher probability of successful memory retrieval, we compared similarity indices in the observed occipital clusters with a 2 (Age Group) × 2 (within vs. between item similarity) × 2 (Memory: remembered/forgotten) × 2 (ROI) mixed factorial ANOVA.

Younger adults showed higher similarity scores compared to older adults ($F(1,65) = 22.25$; $p < .001$) and within-item similarity was generally higher than between-item similarity ($F(1,65) = 435.87$; $p < .001$). In line with the searchlight analysis, the difference between within-item similarity and between-item similarity (i.e. *item specificity*) was smaller in older than in younger adults as indicated by a significant interaction of age and within/between-item similarity ($F(1,65) = 25.05$; $p < .001$; see Figure 7A). Post-hoc tests revealed that within-item similarity (i.e. *item stability*) ($t(65) = 4.94$, $p < .001$) was lower in older adults compared to younger adults, while between-item similarity ($t(65) = 2.16$, $p = .069$) did not differ between age groups after multiple error correction. Within- and between-item similarity differences were not different across ROIs ($F(1,65) = 3.53$; $p = .064$).

Most crucially, subsequently remembered items showed higher similarity scores compared to subsequently forgotten items ($F(1,65) = 7.85$, $p = .007$) which interacted with within/between-item similarity ($F(1,65) = 17.51$; $p < .001$; see Figure 7B). Post-hoc *t*-tests revealed that within-item similarity (i.e. *item stability*) was higher for subsequently remembered than forgotten items ($t(66) = 3.90$, $p < .001$), while there was no difference in between-item similarity ($t(66) = –1.17$, $p = .248$). We found no interaction between memory and age group ($F(1,65) = 3.90$; $p = .052$) or other significant effects (*ps* >.316). Thus, *item stability* was lower in older than in younger adults and supported subsequent recognition performance emphasizing the role of less stable item representations for age-related memory decline.

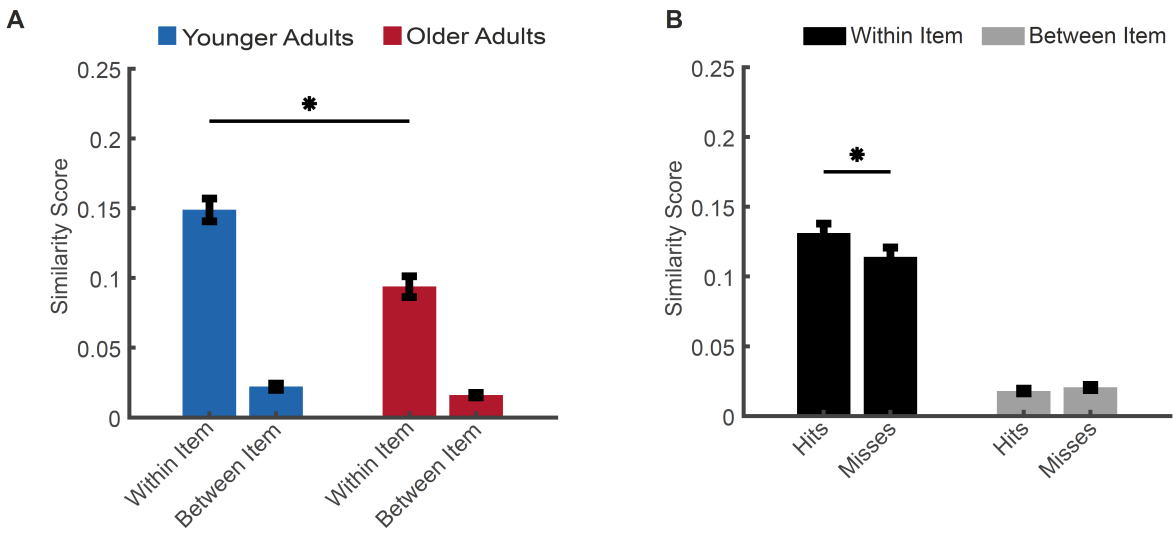

Figure 7. Item representation specificity and memory performance
A. Within-item and between-item similarity in both age groups indicates that lower item specificity in older adults is mostly driven by lower item stability. **B.** Comparing within- and between-item similarity for subsequently remembered items (hits) and not-remembered items (misses) across age groups shows that item stability was higher for later remembered than not-remembered items independent of age.

Discussion

The present fMRI study investigated age differences in the distinctiveness of neural information representations supporting episodic memory performance. We provided a comprehensive account of age differences at different representational levels ranging from *category selectivity* to *item specificity* and *item stability* and delineated their contribution to memory performance in younger and older adults. Combining conventional ROI-based univariate analysis and whole-brain multivariate pattern similarity analysis we demonstrated that age differences in neural distinctiveness coexist at various representational levels, and take the form of reduced category-selective neural processing in VVC regions, and reduced specificity of item representations in occipital areas. A multivariate distinctiveness score revealed the joint contribution of both categorical distinctiveness and item specificity to memory performance and age group differences, with item specificity being the strongest contributor to it. Age differences in occipital item specificity were largely due to reduced item stability across repetitions in older adults, and higher item stability was related to subsequent memory success. Whether or not age differences exist at the item level was a matter of debate that could so far not be settled due to limited evidence (Koen and Rugg, 2019). Our results close this gap in the literature by demonstrating that older adults' neural representation of item-specific information over and above categorical information is indeed reduced compared to younger adults.

Age-related neural dedifferentiation coexists at different representational levels

Previous fMRI studies investigating neural dedifferentiation focused on broader concept representations by assessing univariate category-selective processing (e.g., Park et al., 2004) and/or multivariate category-specific representations (e.g., Carp et al., 2011) in regions of the ventral visual cortex (VVC). In the current study, ROI-based analyses within category-specific regions of interest replicated previous findings: Univariate analyses revealed age-related neural dedifferentiation in terms of reduced category-selective neural processing (e.g., Park et al., 2004), and multivariate pattern similarity analyses revealed reduced categorical specificity (e.g., Carp et al., 2011; Koen et al., 2019) in older compared with younger adults. As predicted by computational models (Li and Sikström, 2002; Li et al., 2000, 2001), age differences in neural category differentiation resulted from neural broadening, that is, increased activation to non-preferred stimuli in the older adults, with no age differences in activation differences for preferred stimuli. More importantly, applying a whole-brain searchlight approach in order to target specificity of neural representations on the item level, we found clear evidence for age differences in item-specific neural activation patterns in occipital regions.

Previous studies with young adults have established that reduced item specificity results in poor memory performance (Hasinski and Sederberg, 2016; Xue et al., 2010), but a pre-defined focus on category-specific regions in VVC (e.g., Koen et al., 2019) may have prevented previous age-comparative studies to reveal age differences in item-level specificity and delineate their role in cognitive decline. The current study demonstrates that age differences in item specificity are most prominent in occipital regions (faces: bilateral intracalcarine cortex, lateral occipital cortex and occipital fusiform cortex; houses: bilateral lingual gyrus, intracalcarine cortex and left occipital fusiform cortex; see Figure 5), that are involved in early visual processing. Together with the fusiform gyrus, lateral occipital cortex has been shown to be critical for visual object (including face) perception (Grill-Spector and Malach, 2004; Grill-Spector et al., 1999; Nagy et al., 2012). Furthermore, the occipital face area, which is connected to the FFA and lateral occipital cortex, constitutes the lowest level in the face perception network and is suggested to represent and integrate facial components (Kadosh et al., 2011; Nagy et al., 2012; Pitcher et al., 2007, 2011). Thus, less precise item-specific activation patterns in older adults in these regions are likely to reflect differences in early processing of the incoming visual information which results in detrimental consequences for downstream (category level) processing. In sum, we argue that our results are in line with core assumptions of computational models (e.g., Li et al., 2001), namely that increased neural variability with age manifests as both degraded item representations in early visual regions and, as a downstream effect, reduced category selectivity in VVC. Hence, we emphasize the important role of item specific and stable neural representations for memory functioning.

Inter- and intraindividual differences in neural distinctiveness are related to memory performance and age

Next, using PLSC, we explored the *joint* contribution of interindividual differences in three measures capturing neural dedifferentiation at three distinct representational levels (*category selectivity*, *category specificity*, and *item specificity*) to memory performance and age. This multivariate analysis revealed that neural distinctiveness was negatively associated with age (neural dedifferentiation) and positively associated with memory performance. In brief, higher dedifferentiation was more common in older adults and low performing individuals. Importantly, of the neural dedifferentiation measures, *item specificity* was the strongest contributor to the associations between neural dedifferentiation, memory, and age. Since the recognition memory task used in the current study required participants to distinguish between highly similar face and house exemplars, rather than simply discriminating faces from houses,

high item specificity was required to perform well. Category selectivity instead may rather be a general indicator of representational quality and a potential downstream effect of item-specific perceptual representations. Thus, while our results nicely illustrate the coexistence of age differences at different representational levels, they clearly identify item specificity in early visual areas as the driving force for interindividual differences in memory performance and age differences.

Our results further revealed the importance of item specificity for the mnemonic fate of single items, that is, subsequent memory effects at the within-person level. In line with others we defined item specificity as the comparison of activation patterns across stimulus repetitions in relation to their similarity to different stimuli of the same category (cf. Hasinski and Sederberg, 2016; Koen and Rugg, 2019; Zheng et al., 2018). In that way, item specificity is a joint effect of representational stability and representational distinctiveness. Thus, theoretically, reduced item specificity in old age may be due to decreased item stability (Zheng et al., 2018), increased within-category similarity (Goh et al. 2010), or both (cf. Koen and Rugg, 2019). However, the computational model by Li et al. (2001) suggests that item-level specificity in older adults is reduced due to increased neural response variability, thus reduced item stability. In line with this proposal, we observed that age difference in item specificity were due to a reduction in item stability in the older age group, whereas no age differences were observed for within-category similarity. Furthermore, item stability displayed an age-independent relation to memory, as indicated by a positive association with recognition probability. Higher item stability in younger compared to older adults in visual regions being related to subsequent memory effects has also been reported by one previous age-comparative study (Zheng et al. 2018), however, the validity of that finding has been questioned (Koen and Rugg, 2019) because age differences in item specificity were not reliable. Our results clearly align with these prior results and highlight that item specificity and item stability are key contributors to age differences in memory performance.

The finding of impoverished item representations in older adults in early visual regions resonates with the long-standing suggestion in cognitive aging science that sensory and cognitive functions are increasingly linked to each other in the course of aging, which further reinforces the close connection of age-related deficits in perceptual processing and declining cognitive abilities (Baltes and Lindenberger, 1997; Li and Lindenberger, 2002; Lindenberger and Baltes, 1994; Schneider and Pichora-Fuller, 2000). The current study substantiates this claim by identifying reduced representational specificity coexisting at different representational

levels but most prominently in early visual regions, which was furthermore linked to inter- and intraindividual differences in memory performance.

Neural dedifferentiation as a consequence of age-related neurotransmitter changes?

In the current study, we proposed that age differences at various representational levels coexist based on a computational model (Li and Sikström, 2002; Li et al., 2000, 2001) that proposes deficient neuromodulation as the causal mechanism for reduced consistency of neural information processing with ensuing consequences for representational distinctiveness and age-related cognitive deficits. Of course, in the current study the precise mechanism underlying the observed representational differences at the various levels remains speculative. Nevertheless, evidence from other studies support the proposal of age differences in neuromodulation as a driving factor for neural dedifferentiation. While the original proposal emphasized age-related changes in dopamine (cf. Abdulrahman et al., 2017; Bäckman et al., 2006, 2010; Li et al., 2001; Rieckmann et al., 2018; Wong et al., 1984), more recently, several studies have revealed the contribution of age-related decline in gamma-aminobutyric acid (GABA) to cognition and neural information representation (cf. Leventhal et al., 2003). For example, using MR spectroscopy to quantify GABA concentrations in occipital voxels, Simmonite et al. (2019) found that lower occipital GABA levels in older adults were associated with declines in fluid processing abilities. Furthermore, Chamberlain et al. (2019; preprint) reported that individual differences in the category specificity of face versus house representations were linked to individual differences in VVC GABA concentrations in older adults, indicating a role of GABA in age-related neural dedifferentiation (see also Cassady et al., 2019; Gagnon et al., 2019; Lalwani et al., 2019). These findings substantiate the key role of proficient (particularly GABAergic) neuromodulation for high-fidelity (i.e., stable and distinct) neural representations and cognitive performance and lay the ground for future studies aiming to understand how age-related deficits in neuromodulation are related to neural dedifferentiation across representational levels.

Conclusion

The present fMRI study set out to investigate age differences in neural information representation and their relation to episodic memory performance. Previous studies have focused on neural dedifferentiation of categorical information but have neglected age differences at the item level. Our results show that differences in representational distinctiveness coexist at various levels and jointly contribute to age-related memory decline.

At the same time, they emphasize the striking relevance of item specificity and item stability for the understanding of inter- and intraindividual differences in memory. Thus, the current study substantiates the claim of a close connection between age differences across processing levels (e.g., sensory and cognitive), as derived from long-standing observations in behavioral aging research. Longitudinal studies are needed to elucidate to what extent the different levels depend on or precede each other and whether a general mechanism (e.g., changes in neuromodulation) accounts for changes in representational properties.

Acknowledgements

This research was conducted within the projects “Lifespan Age Differences in Memory Representations (LIME)” (PI: MCS) and “Lifespan Rhythms of Memory and Cognition (RHYME)” (PI: MWB) at the Max Planck Institute for Human Development. MK received a scholarship from the German Academic Scholarship Foundation. VRS was a fellow of the International Max Planck Research School on the Life Course. MWB was supported by grants from the German Research Foundation (DFG; WE 4269/2-1 and WE 4269/5-1) and an Early Career Research Fellowship by the Jacobs Foundation. MCS was supported by the MINERVA program of the Max Planck Society. We thank all student assistants who helped with data collection, Gabriele Faust, members of the LIME and RHYME projects for helpful feedback, and all study participants for their time.

Author Contributions

MK: Formal analysis, Writing - Original Draft, Writing - Review & Editing, Visualization, VRS: Conceptualization, Software, Investigation, Writing - Original Draft, Writing - Review & Editing, Visualization, AK: Investigation, Writing - Review & Editing, MWB: Conceptualization, Writing - Review & Editing, Supervision, Funding acquisition, Project administration, MCS: Conceptualization, Writing - Original Draft, Writing - Review & Editing, Supervision, Funding acquisition, Project administration

Declaration of Interests

The authors declare no competing interests.

Figure Legends

Figure 1. Task design and schematic of representational similarity levels.

A. The paradigm comprised an encoding (top) and recognition (bottom) task. During encoding, participants were asked to press a button whenever a previously trained target image appeared. During recognition, participants responded via button press whether each presented image was old or new. Here, only sample stimuli from a face block are shown for illustration but also houses and baseline control stimuli were presented. **B.** Illustration of the block design of encoding and recognition tasks. The encoding task consisted of two identical runs, each of which comprised 3 face, 3 house, and 3 baseline (phase-scrambled faces and houses) blocks in alternating and counterbalanced order (either starting with a face or house block). In each block, 20 exemplars of the respective category (face, house, baseline) were presented plus one target stimulus. The recognition task consisted of 3 face and 3 house blocks in alternating and counterbalanced order. In each block, 20 old and 20 new faces/houses were presented. **C.** Simplified illustration of the computed representational similarity levels. For each item presented in encoding run 1, neural pattern similarity was computed as the Pearson correlation of the BOLD pattern elicited by that item and the BOLD pattern(s) elicited by (a) all items of the respective other category in run 1 (between-category similarity), (b) all other items of the same category in run 1 (within-category similarity in run 1), (c) all other items of the same category in run 2 (within-category similarity across runs), (d) the same item in run 2 (within-item similarity; stability). For each subject, the respective similarity measure was averaged across items, resulting in one similarity value for each representational level. Category representation specificity was calculated as the difference of between-category and within-category similarity (b–a). Item representation specificity was calculated as the difference of within-category (across runs) and within-item similarity (d–c). These similarities were assessed based on regions of interests as well as a searchlight approach, see main text.

Figure 2. Identification of category-selective clusters in VVC

Surface rendered illustration of non-overlapping category-selective ROIs across all participants. Purple color indicates face-selective ROI. Green color depicts house-selective ROI. Notably, the face-selective ROI is predominantly located in the lateral ventral visual cortex and the house-selective ROI in the medial VVC closely resembling the category-selective areas observed by Park et al. (2012).

Figure 3. Age differences in category-selective processing during encoding

A. Selectivity score for younger adults (blue; circles) and older adults (red; triangles). Group distributions shown as unmirrored violin plot and boxplots with medians and 95% confidence interval with whiskers representing 2nd and 98th percentiles (Allen et al., 2018). **B.** Neural response to preferred and non-preferred categories within functionally defined VVC ROIs. The neural response is expressed as the averaged *t*-values for preferred/non-preferred categories against phase-scrambled images within the respective ROIs. Error bars indicate standard error of the mean. **C.** Scatterplot illustrating the association between selectivity scores and corrected recognition (*Pr*) over all participants independent of age. Each circle/triangle represents an individual younger/older adult. For illustrative purposes, the best fitting least-squares line is plotted. Significant group differences ($p < .05$) are indicated by asterisk.

Figure 4. Category representation specificity in the VVC

A. Category specificity calculated as the difference between within- and between-category similarity for younger adults (blue; circles) and older adults (red; triangles). Group distributions as unmirrored violin plot and boxplots with medians and 95% confidence interval with whiskers representing 2nd and 98th percentiles. **B.** Pearson correlation of category specificity and corrected recognition (*Pr*) across subjects. For illustrative purposes, the best fitting least-squares line is plotted. Significant group differences ($p < .05$) are indicated by asterisk.

Figure 5. Age differences in item representation specificity and relation to memory performance

A. Significant age differences in item specificity, calculated as the difference between similarity of neural activity patterns across the two repetitions of a given item (i.e.*, item stability)* and the respective within-category similarity, for faces indicated by t-values. Younger adults showed higher item specificity in occipital areas compared to older adults as depicted by the presented cluster. **B.** Significant age differences in item specificity for houses. Again, younger adults showed higher item specificity in occipital areas than older adults. **C.** Pearson correlation of item specificity and corrected recognition (*Pr*) over all subjects (younger adults: blue circles; older adults: red triangles).

Figure 6. A specific profile of neural distinctiveness across representational levels is associated with age and memory performance

A. Profile of latent variable weights (i.e., "brain saliences", e.g., McIntosh et al., 1996) across three neural distinctiveness levels. Red dashed line indicates significance threshold for latent variable weights after multiple error correction. *Z* score-like values of stability suggest a positive relationship between distinctiveness levels as well as age and memory mostly pronounced for occipital item specificity. Using latent variable weights to transform individual empirical distinctiveness measures results in a single latent variable score expressing the largest amount of shared variance between the multivariate pattern of distinctiveness levels as well as age and memory. **B.** In the optimal solution (see Methods), the resulting latent distinctiveness score is positively related to inverted age and **C** memory performance (*Pr*) meaning that higher expression of the distinctiveness profile is related to higher age and worse memory performance (younger adults: blue circles; older adults: red triangles). Note: Age is inverted (the higher the value the younger the participant) in order to create consistent directionality between all variables of interest; see Methods.

Figure 7. Item representation specificity and memory performance

A. Within-item and between-item similarity in both age groups indicates that lower item specificity in older adults is mostly driven by lower item stability. **B.** Comparing within- and between-item similarity for subsequently remembered items (hits) and not-remembered items (misses) across age groups shows that item stability was higher for later remembered than not-remembered items independent of age.

STAR Methods

KEY RESOURCES

REAGENT or RESOURCE	SOURCE	IDENTIFIER
Software and Algorithms		
Fieldtrip Toolbox	http://www.fieldtriptoolbox.org	RRID:SCR_004849
MATLAB 2020b	http://www.mathworks.com	RRID:SCR_001622
Psychtoolbox	http://psychtoolbox.org	RRID:SCR_002881
SPM12	https://www.fil.ion.ucl.ac.uk/spm	RRID:SCR_007037
Fmriprep	http://fmriprep.readthedocs.io	RRID:SCR_016216

Participants

The face-house task described in the current report was embedded in a larger study with an overall sample consisting of 47 younger and 49 older healthy adults who participated in several structural MRI scans and additional behavioral tasks inside and outside the MR scanner. Thirty-nine young and 37 older adults completed the face-house task. We excluded 3 participants (2 young adults and 1 older adult) due to memory performance below chance level and 6 participants (2 young adults and 4 older adults) due to a failure to detect category-selective clusters (see below). Therefore, final analyses were based on a sample of 35 young adults (age: M = 22.11 years, SD = 2.70, 18–27 years; 17 female; 18 male) and 32 older adults (age: M = 70.72 years, SD = 2.26, 67–75 years; 19 female; 13 male) with normal or corrected-to-normal vision and no history of neurological or psychiatric diseases. No participant was taking any medications known to affect brain functions. Furthermore, we screened all older adults with the Mini-Mental State Examination (Folstein et al., 1975) and none scored below the threshold of 26 points (M = 29.19; SD = 1.12; *range* = 26–30). All participants gave written informed consent to take part in the experiment. All procedures were approved by the ethics committee of the German Society for Psychological Research (DGPs).

Stimuli and procedure

Stimulus material. Overall, the stimulus set comprised 300 grey-scale pictures from three different categories: 120 neutral faces (adapted from the FACES database; Ebner et al., 2010), 120 houses (in part adapted from Park et al. 2004 and in part obtained through web search) and 60 phase-scrambled images (30 faces and 30 houses, constructed from randomly chosen pictures of the faces / houses sets) as control stimuli. Face stimuli furthermore consisted of four

subcategories, split by age-group (i.e., young vs. old) and gender (i.e., female vs. male): old-female, old-male, young-female, young-male. Similarly, house stimuli comprised apartment buildings, family houses, sheds and warehouses. In addition, three target stimuli were used for the encoding task, comprising a specific face image, a specific house image and a phase-scrambled image with a white square in the center. All 240 non-target face and house stimuli were split into two sets of 120 items (60 faces and 60 houses comprising 15 stimuli of each subcategory) to present one set during encoding and recognition (old items) and the other set only during recognition (new items). The same item sets were used as old or new items across subjects.

Procedure. Here, we focused on the face-house task consisting of an incidental encoding phase and a surprising recognition test, both conducted inside the MR scanner (see Figure 1A). After verbal and written instructions, giving consent, and performing several behavioral tasks including a short training of the encoding task participants were positioned into the scanner. Here, they again practiced the task for a few trials. The encoding phase consisted of two identical runs including 9 stimulus blocks each (see Figure 1B). Stimuli were presented using Psychtoolbox (Psychophysics Toolbox) for MATLAB (The MathWorks Inc., Natick, MA, USA). During each block, one target (for which participants had to respond) and 20 non-target images of the same category (i.e. faces, houses, or phase-scrambled controls) were presented for 1200 ms with a fixation cross shown between trials (jittered; ranging from 500 ms to 8000 ms). While face or house blocks included five images from each of the four subcategories, phase-scrambled blocks comprised ten scrambled face images and ten scrambled house images. Stimuli were randomly distributed into the blocks. Stimulus order was pseudo-randomized with the restriction that no subcategory appeared twice in a row and the target image was presented neither in the first four nor last four trials of a block. The order of the blocks was alternating and counterbalanced across participants with either starting with a face or house block. Due to a technical failure, the identical stimulus order solution was used for all participants starting with a face block and in 36 participants starting with a house block. To ensure attention to all stimuli during encoding, subjects were instructed to engage in a vigilance task asking them to press a button with their right index finger whenever one of the three target images was presented. Such target trials were excluded from further analyses. In the second run, blocks and trials were exactly repeated as in the first run, i.e. each image was presented twice during encoding. In total, the encoding task lasted 22 minutes.

After encoding, several structural scans were conducted (see below). Then, subjects had a break outside the scanner in which the surprise recognition test was explained to them before

going back into the scanner to perform the recognition test. The recognition test consisted of three face and three house blocks presented in alternated and counterbalanced order. Each block contained 20 previously seen and 20 new images. Subjects were instructed to indicate whether a presented image was old or new via button press during stimulus presentation (1200 ms) or the following grey screen (3000 ms). The order of the trials was pseudo-randomized with the restriction that images of the same subcategory or four old or new images did not appear successively. Furthermore, trials were separated by a jittered fixation cross (500-8000 ms). Again, due to a technical issue an identical stimulus order was used for 13 participants starting with a face block and for 14 participants beginning with a house block. The recognition task lasted about 26 minutes.

Behavioral data analyses

Behavioral data was analyzed using custom-written MATLAB scripts. Performance in the target detection task during encoding was measured as percentage of correct responses to targets. Memory performance in the recognition task was assessed by calculating the discrimination-index *Pr* (Snodgrass and Corwin, 1988), which is an unbiased parameter for recognition performance. *Pr* was calculated as the difference between the hit-rate (proportion of old responses to old images) and the false-alarm-rate (proportion of old responses to new images). We used *t*-tests to probe whether recognition performance was different from chance level, and whether memory performance differed for face and house images. Age differences in memory performance were assessed by computing an independent samples *t*-test between younger and older adults. For effect sizes, we report Cohen's *d*.

fMRI data collection and preprocessing

All MR images were acquired with a 3T Siemens Magnetom Tim Trio scanner. MRI data acquisition included a T1-weighted structural image (MP-RAGE sequence: TR = 2.5 ms, TE = 4.77, flip angle = 7°, TI = 1.1 ms , voxel size = 1 × 1 × 1 mm^3) and T2*-weighted echoplanar images (TR = 2 s, TE = 30 ms, pixel size = 3 × 3 mm^2) sensitive to blood oxygenation level-dependent (BOLD) contrast. EPIs were acquired in two separated encoding and retrieval sessions, which each comprised 270 volumes with 36 axial slices of 3 mm thickness, separated by 3.3 mm. As part of the larger study context, we additionally acquired turbo spin-echo proton density images (PD), diffusion tensor images (DTI) and fluid attenuation inversion recovery (FLAIR).

MRI data were first organized according to "Brain Imaging Data Structure" specifications (BIDS; Gorgolewski et al., 2016). Data processing was performed using the FMRIPrep toolbox (1.4.0) (Esteban et al., 2019) with the default processing steps incorporating the software packages: FSL, FreeSurfer, ANTs and AFNI. First, each T1-weighted volume was corrected for intensity non-uniformity and skull-stripped to reconstruct brain surfaces. Brain-extracted T1-weighted images were spatially normalized to the ICBM 152 Nonlinear Asymmetrical template version 2009c through nonlinear registration. Brain tissue segmentation of cerebrospinal fluid, white-matter and grey-matter was performed on the brain-extracted T1-weighted image. Functional data was slice time corrected, motion corrected and co-registered to the normalized T1-weighted template. For further details including software packages for each preprocessing step in FMRIPrep, please refer to the online documentation under https://fmriprep.org/en/stable/.

For univariate analyses, functional images were resampled to 4 mm isotropic voxels and spatially smoothed with a kernel of 4 mm full width at half maximum. We computed a voxelwise general linear model (GLM) including the first and second encoding run using SPM12. BOLD signal changes were modelled using separate regressors for face, house, and phase-scrambled control image blocks and 6 nuisance motion regressors, which were all convolved with a canonical hemodynamic response function (HRF).

Pattern similarity analyses were conducted on functional images resampled to 2 mm isotropic voxels to enhance signal-to-noise ratio (Dimsdale-Zucker and Ranganath, 2018) and were based on single trial beta weights including one trial specific regressor, one regressor for all other trials, six motion regressors and one run specific mean (Mumford et al., 2012). Trial specific regressors were modelled as a 1.2 second duration delta function convolved with a canonical hemodynamic response function (HRF).

Defining regions of interest

We used a cluster-based approach to define individual functional ROIs most strongly engaged by processing faces or houses during both encoding runs. To restrict our analyses to category-selective processing areas, we defined an anatomical mask of the VVC using the automated anatomical labelling atlas (AAL) including bilateral fusiform gyrus, parahippocampal gyrus and the inferior temporal gyrus (Park et al., 2004). Within this mask, we then contrasted neural responses to face vs. phase-scrambled control image blocks and neural responses to house relative to phase-scrambled control image blocks for each subject. All adjacent voxels exceeding the uncorrected threshold of $p < .005$ were defined as one cluster. As mentioned

above, 2 young and 4 older participants were excluded because clusters included less than 10 voxels. The face-selective ROI was defined as the cluster with the highest averaged t-value for faces compared to phase-scrambled images and the house-selective ROI as the cluster with the highest averaged t-value for houses compared to phase-scrambled images leading to the formation of two individual functional ROIs. Within participants, on average only 4.15% (fusiform gyrus: 4.74%; parahippocampal gyrus: 1.64%; inferior temporal gyrus: 2.40%) of all voxels of the face- and house-selective ROIs overlapped underlining separated category-selective clusters in the VVC.

ROI analysis of category-selective processing

To estimate the neural response magnitude evoked by face and house images within each individual ROI, we first contrasted the BOLD signal elicited by face and house image blocks against the BOLD signal of phase-scrambled control image blocks within the first encoding run. Then, we averaged all *t*-values within each ROI to obtain a standardized neural response value to faces or houses, respectively. Category selectivity scores were computed by contrasting standardized neural responses to the preferred vs. non-preferred image category within each individual ROI, e.g., neural response to faces vs. neural response to houses in the face-selective ROI. To analyze selectivity scores on group-level, we used a 2 (Age Group) × 2 (ROI) mixed factorial ANOVA.

Category selectivity scores were collapsed across ROIs to calculate mean selectivity scores within each participant. This category selectivity score index was correlated with *Pr* across all participants using Pearson correlation. Furthermore, we conducted partial correlations between category selectivity scores and *Pr* with age group as control variable to test whether this relationship is independent of age.

ROI analysis of category representation specificity

To estimate the specificity of neural category representations within category-selective clusters, we compared the within-category similarity to the between-category similarity within the first run using pattern similarity analysis (Kriegeskorte et al., 2008) (see Figure 1C). Within and between-category similarity were calculated separately in both ROIs. Within-category similarity was only calculated for items from the preferred category of the selected area (Koen et al., 2019) and was only computed for items from different blocks to control for potential confounds due to time dependent correlations in hemodynamic responses (Dimsdale-Zucker and Ranganath, 2018). For each item, the within-category similarity was computed as the

average across voxel Pearson correlation of the neural activity pattern of such item to all other items from the same preferred category in a category-selective area (e.g. similarity of a face trial to all other face trials in the face area). For each subject, we averaged within-category similarity across items resulting in one within-category similarity value for each region of interest. The between-category similarity of each item was calculated as the across voxel Pearson correlation of the neural activity pattern of the item to the neural activity pattern of all items from the other category (e.g. similarity of a face trial to all house trials in the face area). We again averaged between-category similarity across items to estimate one between-category similarity value for each region of interest. To test for differences in pattern similarity values, we used a 2 (Age Group) × 2 (within/between-category similarity) × 2 (ROI) mixed factorial ANOVA. To link category specificity and memory performance, we collapsed category specificity across ROIs and calculated zero-order and partial Pearson correlations between category specificity and *Pr* controlled for age.

Searchlight analyses of category representation specificity

We conducted separated searchlight analyses for faces and houses. For each voxel in the brain, we compiled the difference of within- and between-category similarity (i.e., category specificity) within an 8 mm-radius sphere centered on that voxel using modified scripts of the Matlab Toolbox for RSA (Nili et al., 2014). Within and between-category similarity was calculated as described in the previous section. Thus, we derived a whole-brain map for each subject where each value indicated the category specificity of the according sphere.

We used nonparametric, cluster-based, random permutation statistics adapted from the fieldtrip toolbox (Oostenveld et al., 2011) to test for age differences in category specificity across the brain. First, independent *t*-tests were conducted comparing category specificity of young and older adults for each voxel. Adjacent voxels exceeding the defined threshold of $p < .005$ were grouped into clusters. The sum of all *t*-values of these empirical clusters was determined as the respective test statistic. We used the Monte Carlo method to compute a reference distribution for the summed cluster *t*-values. Category specificity of both age groups was randomly assigned (1000 permutations) into two new category specificity sets. In every permutation an independent *t*-test was conducted between the newly generated random sets within each cluster. The sum of these *t*-values during each permutation was included in the estimation of the reference distribution of a cluster.

To correlate category representation specificity and memory performance across participants, we averaged the difference of within- and between-category similarity of each

participant across face and house selective areas. The resulting category specificity score was correlated with *Pr* across participants using Pearson correlations. To control for age, we also calculated partial correlations of the category specificity score and *Pr* with age group as control variable.

Searchlight analyses of item representation specificity

To investigate the specificity of item representations, we compared within-item similarity to between-item similarity (i.e., item specificity) using pattern similarity searchlight analysis (see Figure 1C). Matching the category specificity searchlight analysis, we compiled the within-minus-between item similarity for each voxel within an 8 mm-radius sphere. For each item, within-item similarity was calculated as the across voxel Pearson correlation of the neural activity pattern of a given item from the first encoding run to the neural activity pattern of the same item from the second encoding run in each sphere. Between-item similarity was computed as the correlation of the neural activity pattern of an item of the first encoding run to the neural activity pattern of all other items from the same category of the second encoding run. For each participant, we then averaged within- and between-item similarity across items. We used the resulting within- and between-item similarity brain maps of each participant to calculate one item specificity brain map for each subject. To test for age differences in item specificity across the brain, we used nonparametric, cluster-based, random permutation statistics (see section Searchlight analysis of category representation specificity). First level statistics compared item specificity of young and older adults for each voxel. Second level statistics compared the summed *t*-value of the empirical clusters to a reference distribution computed using the Monte Carlo procedure.

Furthermore, we averaged item specificity for faces and houses for each participant to estimate one item specificity score per participant. Respective item specificity scores were correlated with *Pr* across participants using Pearson correlations and partial correlations to control for age group differences.

Analyzing the multivariate relationship between dedifferentiation on multiple representational levels as well as age and memory performance using PLSC

We performed a PLSC analysis which allows to investigate the joint impact of the multiple distinctiveness levels on age/memory relations (Keresztes et al., 2017; Krishnan et al., 2011; McIntosh et al., 1996). To compile PLSC, we first calculated a between-subject correlation matrix between an n×2-matrix containing standardized age and memory performance (*Pr*) and

an n×3-matrix of neural distinctiveness levels derived from the fMRI analyses (e.g., Garrett et al., 2011). Age was inverted to create consistent directionality between variables of interest. Thus, increasing inverted (= younger) age was positively related to *Pr* indicating better memory performance. The correlation matrix was decomposed using singular value decomposition (SVD) resulting in two latent variables consisting of a diagonal matrix of the correlation strength (i.e., the singular values) and one vector representing the neural distinctiveness profile best describing the brain-age/behavior relationship in our data (distinctiveness weights). We tested the significance of the detected LVs using 10,000 permutations of the singular values corresponding to the LVs which revealed one significant LV ($P < .001$). For the significant LV, we tested the robustness of the distinctiveness weights using a bootstrapping procedure (10,000 resamples). These distinctiveness weights were divided by their respective bootstrapped SE to calculate BSRs as normalized estimates of robustness. Comparable to *z* values, BSRs were considered as reliably robust when below –3 or above 3 which is approximately the level of $p = .05$ after Bonferroni correction (Garret et al., 2011). By calculating the dot product of the model-based distinctiveness weights and each subject's empirical distinctiveness scores, we quantified how much a given individual expresses the profile captured in the LV – the distinctiveness score.

Disentangling the effects of age and memory performance on item specificity

We aimed to disentangle whether lower item representation specificity in older adults occurred due to lower item stability or higher between-item similarity in older adults compared to younger adults and which of these two factors was related to memory performance. Therefore, we averaged within and between-item similarity for later remembered and forgotten items separately in the significant face and house clusters of the conducted searchlight analyses. To test for differences in item similarity, we conducted a 2 (Age Group) × 2 (within-item/within-category similarity) × 2 (Memory: remembered/forgotten) × 2 (ROI) mixed factorial ANOVA.

Resource availability

Data and Code for all analysis of this manuscript will be made publicly available on osf upon publication.

References

Abdulrahman, H., Fletcher, P.C., Bullmore, E., and Morcom, A.M. (2017). Dopamine and memory dedifferentiation in aging. NeuroImage *153*, 211–220.

Allen, M., Poggiali, D., Whitaker, K., Marshall, T.R., and Kievit, R. (2018). Raincloud plots: a multi-platform tool for robust data visualization. PeerJ Preprints 6:e27137v1. doi: https://doi.org/10.7287/peerj.preprints.27137v1

Bäckman, L., Nyberg, L., Lindenberger, U., Li, S.-C., and Farde, L. (2006). The correlative triad among aging, dopamine, and cognition: current status and future prospects. Neuroscience & Biobehavioral Reviews *30*, 791–807.

Bäckman, L., Lindenberger, U., Li, S.-C., and Nyberg, L. (2010). Linking cognitive aging to alterations in dopamine neurotransmitter functioning: recent data and future avenues. Neuroscience & Biobehavioral Reviews *34*, 670–677.

Baltes, P.B., and Lindenberger, U. (1997). Emergence of a powerful connection between sensory and cognitive functions across the adult life span: a new window to the study of cognitive aging? Psychology and Aging *12*, 12–21.

Carp, J., Park, J., Polk, T.A., and Park, D.C. (2011). Age differences in neural distinctiveness revealed by multi-voxel pattern analysis. NeuroImage *56*, 736–743.

Cassady, K., Gagnon, H., Lalwani, P., Simmonite, M., Foerster, B., Park, D., Peltier, S.J., Petrou, M., Taylor, S.F., Weissman, D.H., et al. (2019). Sensorimotor network segregation declines with age and is linked to GABA and to sensorimotor performance. NeuroImage *186*, 234–244.

Chamberlain, J.D., Gagnon, H., Lalwani, P., Cassady, K.E., Simmonite, M., Foerster, B.R., Petrou, M., Seidler, R.D., Taylor, S.F., Weissman, D.H., et al. (2019). GABA levels in ventral visual cortex decline with age and are associated with neural distinctiveness. BioRxiv 743674. doi: https://doi.org/10.1101/743674

Dimsdale-Zucker, H.R., and Ranganath, C. (2018). Representational similarity analyses: A practical guide for functional MRI applications. In Handbook of Behavioral Neuroscience, D. Manahan-Vaughan, ed., pp. 509–525.

Ebner, N.C., Riediger, M., and Lindenberger, U. (2010). FACES—A database of facial expressions in young, middle-aged, and older women and men: Development and validation. Behavior Research Methods *42*, 351–362.

Edelman, S. (1998). Representation is representation of similarities. Behavioral and Brain Sciences *21*, 449–467.

Epstein, R., and Kanwisher, N. (1998). A cortical representation of the local visual environment. Nature *392*, 598–601.

Esteban, O., Markiewicz, C.J., Blair, R.W., Moodie, C.A., Isik, A.I., Erramuzpe, A., Kent, J.D., Goncalves, M., DuPre, E., Snyder, M., et al. (2019). fMRIPrep: a robust preprocessing pipeline for functional MRI. Nature Methods *16*, 111–116.

Folstein, M.F., Folstein, S.E., and McHugh, P.R. (1975). "Mini-mental state": A practical method for grading the cognitive state of patients for the clinician. Journal of Psychiatric Research *12*, 189–198.

Gagnon, H., Simmonite, M., Cassady, K., Chamberlain, J., Freiburger, E., Lalwani, P., Kelley, S., Foerster, B., Park, D.C., Petrou, M., et al. (2019). Michigan Neural Distinctiveness (MiND) study protocol: investigating the scope, causes, and consequences of age-related neural dedifferentiation. BMC Neurology *19*, 61.

Garrett, D.D., Kovacevic, N., McIntosh, A.R., and Grady, C.L. (2011). The importance of being variable. The Journal of Neuroscience *31*, 4496–4503.

Gorgolewski, K.J., Auer, T., Calhoun, V.D., Craddock, R.C., Das, S., Duff, E.P., Flandin, G., Ghosh, S.S., Glatard, T., Halchenko, Y.O., et al. (2016). The brain imaging data structure, a format for organizing and describing outputs of neuroimaging experiments. Scientific Data *3*, 160044.

Grill-Spector, K., and Malach, R. (2004). The human visual cortex. Annual Review of Neuroscience *27*, 649–677.

Grill-Spector, K., Kushnir, T., Edelman, S., Avidan, G., Itzchak, Y., and Malach, R. (1999). Differential processing of objects under various viewing conditions in the human lateral occipital complex. Neuron *24*, 187–203.

Hasinski, A.E., and Sederberg, P.B. (2016). Trial-level information for individual faces in the fusiform face area depends on subsequent memory. NeuroImage *124*, 526–535.

Haynes, J.-D., and Rees, G. (2006). Decoding mental states from brain activity in humans. Nature Reviews Neuroscience *7*, 523–534.

Kadosh, K.C., Walsh, V., and Kadosh, R.C. (2011). Investigating face-property specific processing in the right OFA. Social Cognitive and Affective Neuroscience *6*, 58–65.

Kanwisher, N., McDermott, J., and Chun, M.M. (1997). The fusiform face area: A module in human extrastriate cortex specialized for face perception. Journal of Neuroscience *17*, 4302–4311.

Keresztes, A., Bender, A.R., Bodammer, N.C., Lindenberger, U., Shing, Y.L., and Werkle-Bergner, M. (2017). Hippocampal maturity promotes memory distinctiveness in childhood and adolescence. Proceedings of the National Academy of Sciences of the United States of America *114*, 9212–9217.

Koen, J.D., and Rugg, M.D. (2019). Neural dedifferentiation in the aging brain. Trends in Cognitive Sciences *23*, 547–559.

Koen, J.D., Hauck, N., and Rugg, M.D. (2019). The relationship between age, neural differentiation, and memory performance. The Journal of Neuroscience *39*, 149–162.

Koen, J.D., Srokova, S., and Rugg, M.D. (2020). Age-related neural dedifferentiation and cognition. Current Opinion in Behavioral Sciences *32*, 7–14.

Kriegeskorte, N., Formisano, E., Sorger, B., and Goebel, R. (2007). Individual faces elicit distinct response patterns in human anterior temporal cortex. Proceedings of the National Academy of Sciences of the United States of America *104*, 20600–20605.

Kriegeskorte, N., Mur, M., and Bandettini, P.A. (2008). Representational similarity analysis - connecting the branches of systems neuroscience. Frontiers in Systems Neuroscience *2*, 4.

Krishnan, A., Williams, L.J., McIntosh, A.R., and Abdi, H. (2011). Partial Least Squares (PLS) methods for neuroimaging: A tutorial and review. NeuroImage *56*, 455–475.

Lalwani, P., Gagnon, H., Cassady, K., Simmonite, M., Peltier, S., Seidler, R.D., Taylor, S.F., Weissman, D.H., and Polk, T.A. (2019). Neural distinctiveness declines with age in auditory cortex and is associated with auditory GABA levels. NeuroImage *201*, 116033.

Leventhal, A.G., Wang, Y., Pu, M., Zhou, Y., and Ma, Y. (2003). GABA and its agonists improved visual cortical function in senescent monkeys. Science *300*, 812–815.

Li, K.Z.H., and Lindenberger, U. (2002). Relations between aging sensory/sensorimotor and cognitive functions. Neuroscience & Biobehavioral Reviews *26*, 777–783.

Li, S.-C., and Sikström, S. (2002). Integrative neurocomputational perspectives on cognitive aging, neuromodulation, and representation. Neuroscience & Biobehavioral Reviews *26*, 795–808.

Li, S.-C., Lindenberger, U., and Frensch, P.A. (2000). Unifying cognitive aging: From neuromodulation to representation to cognition. Neurocomputing *32–33*, 879–890.

Li, S.-C., Lindenberger, U., and Sikström, S. (2001). Aging cognition: From neuromodulation to representation. Trends in Cognitive Sciences *5*, 479–486.

Lindenberger, U., and Baltes, P.B. (1994). Sensory functioning and intelligence in old age: a strong connection. Psychology and Aging *9*, 339–355.

McIntosh, A.R., Bookstein, F.L., Haxby, J.V., and Grady, C.L. (1996). Spatial pattern analysis of functional brain images using partial least squares. NeuroImage *3*, 143–157.

Mumford, J.A., Turner, B.O., Ashby, F.G., and Poldrack, R.A. (2012). Deconvolving BOLD activation in event-related designs for multivoxel pattern classification analyses. NeuroImage *59*, 2636–2643.

Mur, M., Bandettini, P.A., and Kriegeskorte, N. (2009). Revealing representational content with pattern-information fMRI—an introductory guide. Social Cognitive and Affective Neuroscience *4*, 101–109.

Nagy, K., Greenlee, M.W., and Kovács, G. (2012). The lateral occipital cortex in the face perception network: An effective connectivity study. Frontiers in Psychology *3*, 141.

Nili, H., Wingfield, C., Walther, A., Su, L., Marslen-Wilson, W., and Kriegeskorte, N. (2014). A toolbox for representational similarity analysis. PLoS Computational Biology *10,* e1003553.

Paller, K.A., and Wagner, A.D. (2002). Observing the transformation of experience into memory. Trends in Cognitive Sciences *6*, 93–102.

Park, D.C., Polk, T.A., Park, R., Minear, M., Savage, A., and Smith, M.R. (2004). Aging reduces neural specialization in ventral visual cortex. Proceedings of the National Academy of Sciences of the United States of America *101*, 13091–13095.

Park, J., Carp, J., Hebrank, A., Park, D.C., and Polk, T.A. (2010). Neural specificity predicts fluid processing ability in older adults. Journal of Neuroscience *30*, 9253–9259.

Park, J., Carp, J., Kennedy, K.M., Rodrigue, K.M., Bischof, G.N., Huang, C.-M., Rieck, J.R., Polk, T.A., and Park, D.C. (2012). Neural broadening or neural attenuation? Investigating age-related dedifferentiation in the face network in a large lifespan sample. Journal of Neuroscience *32*, 2154–2158.

Payer, D., Marshuetz, C., Sutton, B., Hebrank, A., Welsh, R.C., and Park, D.C. (2006). Decreased neural specialization in old adults on a working memory task. Neuroreport *17*, 487–491.

Pitcher, D., Walsh, V., Yovel, G., and Duchaine, B. (2007). TMS evidence for the involvement of the right occipital face area in early face processing. Current Biology *17*, 1568–1573.

Pitcher, D., Walsh, V., and Duchaine, B. (2011). The role of the occipital face area in the cortical face perception network. Experimental Brain Research *209*, 481–493.

Rieckmann, A., Johnson, K.A., Sperling, R.A., Buckner, R.L., and Hedden, T. (2018). Dedifferentiation of caudate functional connectivity and striatal dopamine transporter density predict memory change in normal aging. Proceedings of the National Academy of Sciences of the United States of America *115*, 10160–10165.

Schneider, B.A., and Pichora-Fuller, M.K. (2000). Implications of perceptual deterioration for cognitive aging research. In The Handbook of Aging and Cognition, 2nd Ed, (Mahwah, NJ, US: Lawrence Erlbaum Associates Publishers), pp. 155–219.

Simmonite, M., Carp, J., Foerster, B.R., Ossher, L., Petrou, M., Weissman, D.H., and Polk, T.A. (2019). Age-related declines in occipital GABA are associated with reduced fluid processing ability. Academic Radiology *26*, 1053–1061.

Snodgrass, J.G., and Corwin, J. (1988). Pragmatics of measuring recognition memory: Applications to dementia and amnesia. Journal of Experimental Psychology: General *117*, 34–50.

Sommer, V.R., Fandakova, Y., Grandy, T.H., Shing, Y.L., Werkle-Bergner, M., and Sander, M.C. (2019). Neural pattern similarity differentially relates to memory performance in younger and older adults. Journal of Neuroscience *39*, 8089–8099.

Srokova, S., Hill, P.F., Koen, J.D., King, D.R., and Rugg, M.D. (2020). Neural differentiation is moderated by age in scene- but not face-selective cortical regions. ENeuro *7*, 3.

St-Laurent, M., Abdi, H., Bondad, A., and Buchsbaum, B.R. (2014). Memory reactivation in healthy aging: Evidence of stimulus-specific dedifferentiation. Journal of Neuroscience *34*, 4175–4186.

Trelle, A.N., Henson, R.N., and Simons, J.S. (2019). Neural evidence for age-related differences in representational quality and strategic retrieval processes. Neurobiology of Aging *84*, 50–60.

Voss, M.W., Erickson, K.I., Chaddock, L., Prakash, R.S., Colcombe, S.J., Morris, K.S., Doerksen, S., Hu, L., McAuley, E., and Kramer, A.F. (2008). Dedifferentiation in the visual cortex: An fMRI investigation of individual differences in older adults. Brain Research *1244*, 121–131.

Wong, D.F., Wagner, H.N., Dannals, R.F., Links, J.M., Frost, J.J., Ravert, H.T., Wilson, A.A., Rosenbaum, A.E., Gjedde, A., Douglass, K.H., et al. (1984). Effects of age on dopamine and serotonin receptors measured by positron tomography in the living human brain. Science *226*, 1393–1396.

Xue, G. (2018). The neural representations underlying human episodic memory. Trends in Cognitive Sciences *22*, 544–561.

Xue, G., Dong, Q., Chen, C., Lu, Z., Mumford, J.A., and Poldrack, R.A. (2010). Greater neural pattern similarity across repetitions is associated with better memory. Science *522*, 97–101.

Zheng, L., Gao, Z., Xiao, X., Ye, Z., Chen, C., and Xue, G. (2018). Reduced fidelity of neural representation underlies episodic memory decline in normal aging. Cerebral Cortex *28*, 2283–2296.